THE PHOTOGRAMMETRIC RECORD

The Photogrammetric Record 28(141): 86–95 (March 2013)
DOI: 10.1111/phor.12009

CORRELATION ANALYSIS OF CAMERA SELF-CALIBRATION IN CLOSE RANGE PHOTOGRAMMETRY

RONGFU TANG (rongfu.tang@ifp.uni-stuttgart.de)
DIETER FRITSCH (dieter.fritsch@ifp.uni-stuttgart.de)
University of Stuttgart,Germany

Abstract

While the Brown self-calibration model has been widely used in close range photogrammetry for over 40 years, the negative effects of the well-known high correlations between parameters are not clear. This paper presents a novel view and study of these correlations, which are shown to be inherent in the Brown model due to its polynomial nature; they occur exactly as with additional parameters in aerial photogrammetry. Although it has high correlations with the decentring distortion parameters, the principal point can be located precisely (up to a few pixels) in self-calibration with an appropriate image configuration. An alternative model of the in-plane distortion is proposed, which helps to reduce the correlation with principal distance.

KEYWORDS: camera self-calibration, close range photogrammetry, decentring distortion, high correlations, in-plane distortion, principal point

INTRODUCTION

CAMERA CALIBRATION is an essential subject in photogrammetry and computer vision. Self-calibration by using additional parameters has been widely accepted and routinely used as an efficient technique in close range photogrammetry. Notwithstanding any changes of terminology, the self-calibration model proposed by D. C. Brown (1966, 1971) has remained virtually unchallenged for over 40 years (Clarke and Fryer, 1998). The Brown self-calibration model includes the three interior orientation (IO) parameters, the radial distortion and the decentring distortion parameters. The three IO parameters are given as

$$\Delta x_i = \Delta x_0 - \bar{x}\Delta f/f \tag{1}$$

$$\Delta y_i = \Delta y_0 - \bar{y}\Delta f/f \tag{2}$$

where f is the principal distance, and $\bar{x}$ and $\bar{y}$ are the image coordinates. The three IO parameters Δx_0, Δy_0 and Δf stand for principal point shift and principal distance variation.

The radial distortion is represented as follows:

$$\Delta r = K_1 r^3 + K_2 r^5 + K_3 r^7 \tag{3}$$

$$\Delta x_r = \bar{x}\Delta r/r,\ \Delta y_r = \bar{y}\Delta r/r \tag{4}$$

where K_1, K_2 and K_3 are the coefficients of three odd-order terms, and $r^2 = \bar{x}^2 + \bar{y}^2$.

The decentring distortion is given in the following equations with two coefficients, P_1 and P_2:

$$\Delta x_d = P_1(r^2 + 2\bar{x}^2) + 2P_2\overline{xy} = P_1(3\bar{x}^2 + \bar{y}^2) + 2P_2\overline{xy} \tag{5}$$

$$\Delta y_d = 2P_1\overline{xy} + P_2(r^2 + 2\bar{y}^2) = 2P_1\overline{xy} + P_2(\bar{x}^2 + 3\bar{y}^2). \tag{6}$$

This classic Brown model has seen great significance in computer vision as well (Weng et al., 1992; Zhang, 2000). The zoom effects of the Brown model were observed in self-calibration by many researchers (Wiley and Wong, 1995; Fraser and Al-Ajlouni, 2006).

Besides the radial and decentring distortion, the out-of-plane and in-plane distortion were discussed in close range applications (Fraser, 1997). The in-plane distortion, given in the following equation, was suggested to be combined with the Brown model for digital camera self-calibration:

$$\Delta x_f = B_1\bar{x} + B_2\bar{y} \tag{7}$$

where B_1 and B_2 are called the affinity and the shear terms, respectively. They account for differential scaling and non-orthogonality between two image axes, respectively.

This 10-parameter model (Δx_0, Δy_0, Δf, K_1, K_2, K_3, P_1, P_2, B_1 and B_2) is currently the most favourable one for camera self-calibration. It is efficient and powerful, enabling the calibration of a huge range of lenses. However, one of its main disadvantages is the high correlations between different parameters. The high correlations have been well recognised for almost as long as the self-calibration itself (Brown, 1971; 1972; Ziemann, 1986; Fraser, 1997; Clarke and Fryer, 1998; Clarke et al., 1998; Luhmann et al., 2006). Three types of high correlations are usually of major concern in photogrammetry. They are:

(1) the correlations between the IO and the exterior orientation (EO) parameters;
(2) the correlations between the principal point and the decentring parameters P_1 and P_2; and
(3) the correlations between Δf and the in-plane distortion parameter B_1.

On the one hand, while the first type's correlations can be quite severe for calibrating cameras with a long focal length (Stamatopoulos and Fraser, 2011), they are negligible in most other cases as long as the image configurations are appropriate (Luhmann et al., 2006). On the other hand, the high correlations of the second and the third types are often encountered in practice. The correlations between the principal point and the decentring parameters are usually higher than 0·90.

High correlations indicate that the errors of one parameter can be partially "corrected" by the parameter it is correlated with. High correlations between the principal point and the decentring parameters imply that the decentring distortion can be partially compensated by the principal point, and vice versa. This effect is unfavourable and may

lead to negative effects in self-calibration. For example, high correlations can result in a weak, or even false, calibration solution. Even worse, the calibration results might be block-dependent.

By considering the importance of the principal point, many studies were undertaken in the early years of implementing the Brown model to avoid high correlations. However, most of them seemed unnecessary (see Clarke and Fryer, 1998, for a review). In this work, the study of high correlations of the second and the third types in camera self-calibration is revisited. A novel mathematical view of the high correlations is proposed. The potentially harmful effects of these high correlations are investigated. Moreover, an alternative model of the in-plane distortion is proposed to reduce the correlations between B_1 and Δf. Since plumb-line calibration is unable to locate the principal point (Clarke and Fryer, 1998; Lerma and Cabrelles, 2007) and the decentring parameters are rarely applied in long focal length camera calibration (Stamatopoulos and Fraser, 2011), these two cases are beyond the current study and are not considered further.

High Correlations in Polynomial Models

It was illustrated in Clarke et al. (1998) that the EO parameters were linked to the high correlations between the principal point and the decentring parameters. However, there were only four images in their simulation configuration (which may be inappropriate) and their conclusion is unlikely to be true. It can be shown that, even if the EO parameters are independently observed or precisely given, high correlations still remain between the principal point and the decentring parameters. Thus, the EO parameters should not be considered to be the main factor causing the high correlations. In fact, this work will show that the high correlations are inherently caused by the polynomial nature of the Brown model, independently of the EO parameters.

For this purpose, it is interesting to shift the focus somewhat to the polynomial self-calibration models in aerial photogrammetry. These polynomial models (or additional parameters, APs) were quite often employed to compensate the distortion of airborne cameras. The polynomial APs of the second and fourth orders were put forward by Ebner (1976) and Gruen (1978), respectively. The polynomial APs were recently reconsidered and the so-called Legendre self-calibration APs were presented in Tang et al. (2012). The Legendre APs can be considered as a superior generalisation of the models proposed by Ebner and Gruen. The mathematical principles of all the polynomial APs are based on function approximation and the Weierstrass theorem (Tang et al., 2012).

The first five terms of the two-dimensional polynomial are given in the following equations, by neglecting the scale and constant terms which are entirely irrelevant to correlation analyses:

$$\begin{aligned} \Delta x_P &: a_1\bar{x} + a_2\bar{y} + a_3\overline{xy} + a_4\bar{x}^2 + a_5\bar{y}^2 \\ \Delta y_P &: b_1\bar{x} + b_2\bar{y} + b_3\overline{xy} + b_4\bar{x}^2 + b_5\bar{y}^2 \end{aligned} \tag{8}$$

where Δx_P and Δy_P denote the polynomials, and a_i and b_i (i = 1, 2, …,5) are the coefficients. Four coefficients must be eliminated due to the high correlations. In particular, a_1 and b_2 are highly correlated in the presence of Δf; a_2 and b_1 are highly correlated due to the exterior orientation rotations; a_4 and b_3 are highly correlated in the presence of Δx_0; and a_3 and b_5 are highly correlated in the presence of Δy_0. Thus the first five terms of the

two polynomial AP equations, obtained after the elimination of these highly correlated terms, are shown as

$$\begin{aligned} \Delta x_P &: a_1\bar{x} + a_2\bar{y} + a_3\overline{xy} + a_4\bar{x}^2 + a_5\bar{y}^2 \\ \Delta y_P &: a_2\bar{x} + (-a_1)\bar{y} + (-a_4)\overline{xy} + b_4\bar{x}^2 + (-a_3)\bar{y}^2. \end{aligned} \tag{9}$$

Note that the decentring distortion parameters are $3P_1\bar{x}^2$ and $2P_1\overline{xy}$, and $3P_2\bar{y}^2$ and $2P_2\overline{xy}$ in the Brown model (equations (5) and (6)), while the corresponding terms in equations (9) are $a_4\bar{x}^2$ and $-a_4\overline{xy}$, and $-a_3\bar{y}^2$ and $a_3\overline{xy}$, respectively. The signs of the terms in $\overline{xy}$ in the Brown model are different from those in equations (9). It is stressed that these *sign distinctions* are the reason causing the high correlations between the principal point and the decentring parameters. In order to quantitatively illustrate the effects of these distinctions, two alternative formulae of the Brown decentring distortion equations (5) and (6) are given in the equations below, following the spirit of equations (9). The first two formulae remove the $\overline{xy}$ terms, while the second two change the signs of the $\overline{xy}$ terms:

$$\begin{aligned} \Delta x_d &= P_1(3\bar{x}^2 + \bar{y}^2) \\ \Delta y_d &= P_2(\bar{x}^2 + 3\bar{y}^2) \end{aligned} \tag{10}$$

$$\begin{aligned} \Delta x_d &= P_1(3\bar{x}^2 + \bar{y}^2) - 2P_2\bar{x}\bar{y} \\ \Delta y_d &= P_2(\bar{x}^2 + 3\bar{y}^2) - 2P_1\bar{x}\bar{y}. \end{aligned} \tag{11}$$

The correlations of these formulae and the decentring distortion model (equations (5) and (6)) are evaluated in simulation studies, where a 10-image and a four-image configuration are employed, as depicted in Fig. 1. In the 10-image configuration, there are eight images around a 3D testfield with a convergent angle of approximately 45° and two looking vertically down. This highly redundant and reliable configuration follows the suggestions in Wester-Ebbinghaus (1983) and Luhmann et al. (2006). The four-image view is similar to that used in Clark et al. (1998), with a convergent angle of approximately 90°. The focal length of the virtual lens is 8 mm and the image format is 7 mm × 7 mm. The standard deviation of the Gaussian noise in the image measurements is 0·1 pixel. The IO parameters of non-zero Δx_0, Δy_0, Δf and K_1, plus $K_2 = K_3 = P_1 = P_2 = 0$, are introduced into the simulated camera. The self-calibration models in equations (3) to (6) are adopted in the self-calibration adjustment, together with different formulae of the decentring distortion, namely, equations (5), (6), (10) and (11). The EO parameters are precisely given in the adjustment.

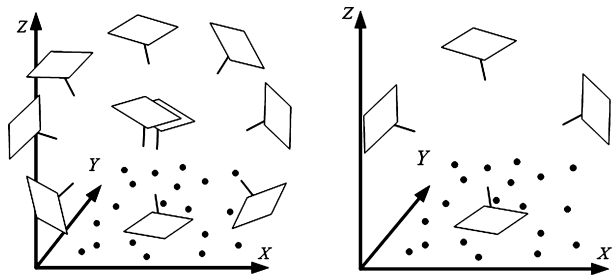

FIG. 1. Self-calibration configurations of 10 images (left) and four images (right).

TABLE 1. Correlations between the principal point and the decentring distortion using different formulae.

$(\Delta x_0 - P_1)/(\Delta y_0 - P_2)$	*Equations (5) and (6)*	*Equations (10)*	*Equations (11)*
10-image configuration	0·94/0·92	0·63/0·66	0·30/0·33
4-image configuration	0·91/0·87	0·69/0·43	0·39/0·04

The correlations between Δx_0 and P_1, and between Δy_0 and P_2 are depicted in Table 1. It is clear that equations (10) obtain smaller correlations than the original Brown formulae (5) and (6). Furthermore, equations (11), which somewhat resemble the polynomial model (9), deliver the lowest correlations in both configurations. It reduces remarkably the correlations from over 0·90 to a much lower level, around 0·30 or even smaller.

Therefore, the high correlations between Δx_0 and P_1, and between Δy_0 and P_2 are due to the sign difference between equations (5), (6) and (9). In other words, these high correlations are essentially caused by the *polynomial representation* of the decentring distortion in the Brown model. High correlations in the polynomial self-calibration models are a distinctive characteristic of the camera interior orientation, and they are nearly independent of the exterior orientation and the block geometry. These high correlations are exactly those which occurred in the polynomial APs in aerial photogrammetry. This is an interesting link between the Brown model in close range photogrammetry and the polynomial self-calibration models in aerial photogrammetry.

The high correlation between Δf and B_1 is again due to the polynomial representation. Following the spirit of equations (9), the alternative formulae of the in-plane distortion are given as

$$\begin{aligned} \Delta x_f &= B_1\bar{x} + B_2\bar{y} \\ \Delta y_f &= -B_1\bar{y}. \end{aligned} \tag{12}$$

Equations (12) handle the scaling effect in a similar way to equation (7); their geometric interpretation is illustrated in Fig. 2. The advantage of equations (12) is that they always deliver a lower correlation between B_1 and Δf than equation (7), without increasing the risk of overparameterisation.

PRINCIPAL POINT LOCATION

As high correlations between the principal point and the decentring parameters are intrinsic in the Brown model, it is necessary to quantitatively investigate to what extent the principal point can compensate the decentring distortion.

The effects of the high correlations on calibration were studied in simulation experiments. The virtual camera is the same as the one in the last section. To ensure a reliable and highly redundant calibration geometry, the 10-image configuration (Fig. 1(left)) was

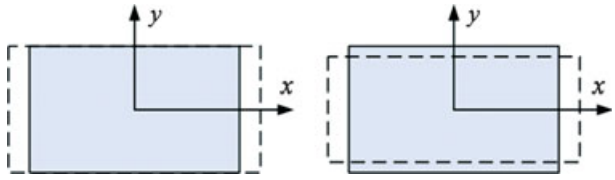

FIG. 2. The geometric effects of the affinity parameters $B_1 > 0$ in equations (7) (left) and (12) (right).

adopted. The non-zero radial and decentring distortions were introduced into the camera. Considering that the decentring distortion rarely exceeds 10 μm at the extremity of the image format in digital cameras (Fraser, 1997), the imposed decentring distortion increased gradually from 1 to 10 μm.

Two strategies of self-calibration adjustment were performed. In the first strategy, the three IO parameters (Δx_0, Δy_0 and Δf) and the radial distortion parameters were employed; while the second strategy additionally used the decentring parameters. The first strategy was designed to demonstrate to what extent the decentring distortion can be compensated by the parameters of the principal point, while the second strategy was intended to show the interaction between the principal point and the decentring parameters in the calibration due to high correlations.

The results of the two adjustment strategies are illustrated in Figs. 3 and 4, respectively, where the errors of the principal point and principal distance, and a posteriori sigma zero, are depicted. The a posteriori sigma zero, denoted by $\hat{\sigma_0}$, indicates the a posteriori estimate of the standard deviation of the noise.

From Fig. 3, it can be seen that the errors of the principal point calibration grow with the increasing decentring distortion. This implies that uncompensated decentring distortion does impact upon the principal point location due to their high correlation. On the other hand, it is certain from the increasing $\hat{\sigma_0}$ that the decentring distortion cannot be entirely compensated by the principal point. This uncompensated effect can be observed when the $\hat{\sigma_0}$ estimate is significantly larger than 0·1 pixel. It corresponds to the maximum value of the decentring distortion being over 3 μm and the principal point deviation being over 3 pixels in Fig. 3(left). In other words, a principal point variation of smaller than 3 pixels may be undetectable in the self-calibration, due to the high correlations with the decentring distortion parameters. It is also interesting to note that the errors in the principal distance are smaller than 1 pixel, and independent of the varying decentring distortion. This must be attributed to the very small correlations between the principal distance and the decentring parameters.

In the experiments of the second strategy, the correlations between Δx_0 and P_1, and between Δy_0 and P_2, are over 0·92 and are independent of the values of the decentring distortion. The errors of the principal point location are rarely larger than 1 pixel. The $\hat{\sigma_0}$ estimate is close to the true value (0·1 pixel) and is fully independent of the varying decentring distortion. These results (Fig. 4) show that the interaction between the principal point and the decentring parameters are trivial in self-calibration with an appropriate image configuration.

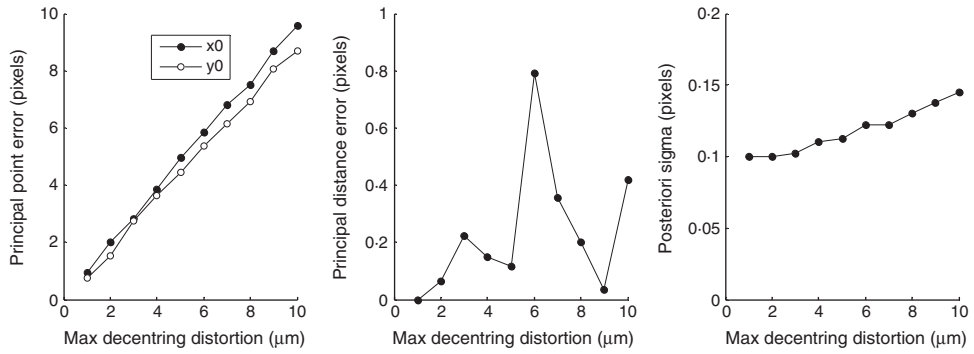

FIG. 3. The variations of principal point (left), principal distance (middle) and $\hat{\sigma_0}$ (right) with the uncompensated decentring distortion.

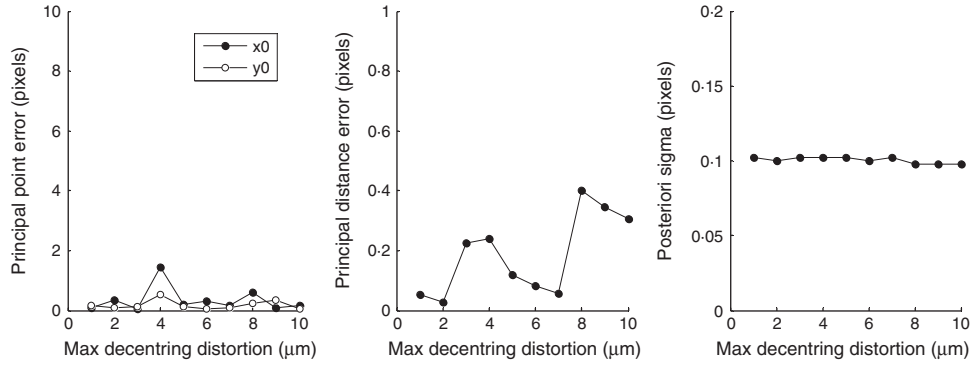

FIG. 4. The variations of principal point (left), principal distance (middle) and $\hat{\sigma}_0$ (right) with different decentring distortion (by using the decentring parameters in self-calibration).

The focal length of the simulation camera was also changed to 20 mm and the experiments were repeated. Similar results to the 8 mm simulation were obtained. It can therefore be safely concluded that, although high correlations do exist with the decentring distortion parameters, the error of the principal point location, which rarely exceeds 1 pixel in the present studies, is insignificant. In other words, the principal point can be reliably and precisely located in self-calibration under appropriate image configurations. This is a very encouraging result. It may be a reason why the Brown model has worked so well in practice, even though high correlations exist between different parameters. As the negative effects of high correlations are insignificant, the early work which attempted to circumvent the high correlations may be unnecessary. In fact, the current experiments suggest that the decentring distortion parameters should be employed in self-calibration whenever possible. The use of the decentring parameters not only reduces the residuals of the image observations, but it also improves the accuracy of the principal point location when significant decentring distortion is present.

The precision in the location of the principal point, which may be unsurprising, can be attributed to several factors. Firstly, it should be noted that, although high correlations do cause the risk of miscalibration, it usually depends on the particular circumstances whether the amount of miscalibration is practically significant. On the one hand, a high correlation mathematically implies a significant linear relation between two parameters. On the other hand, the quantitative influence of one parameter on another depends on many factors, such as the magnitudes of the parameters and the scaling factor (geometrically, the gradient of the linear dependence). The scaling factor of the linear correlations between Δx_0 and P_1, and between Δy_0 and P_2, might be small (though this is not proved here). The limited magnitude of the decentring distortion, which is usually smaller than 10 μm at the periphery of the image, is also beneficial for decreasing the potential negative effects of high correlations. Secondly, the terms $P_1\bar{y}^2$ and $P_2\bar{x}^2$ in equations (5) and (6) are helpful for decorrelation and determining the principal point location.

IN-PLANE DISTORTION

In this section, the empirical experiments carried out to demonstrate the performance of the alternative formulae (12) of the in-plane distortion are discussed.

Two simulated and one practical experiment were performed, denoted by "simulation-10", "simulation-4" and "practical-10", respectively. The first simulation included 10 images with a similar configuration to Fig. 1(left), and the second includes four images whose distribution is akin to Fig. 1(right). Values of $\Delta f = 50\,\mu m$ and $B_1 = B_2 = 0$ were used for the virtual cameras in both simulation experiments. The uEye camera (12 mm focal length) of Imaging Development System (IDS) GmbH was used in the "practical-10" experiments. The self-calibration results are depicted in Table 2, where the correlation between B_1 and Δf is denoted by R_{fB}.

In both simulation experiments, equations (7) and (12) gave the same $\hat{\sigma}_0$ and a similar Δf. The slight refinements of Δf and R_{fB} are observed by using equations (12), particularly in the case of "simulation-4" where the configuration is weak. The refined performance of equations (12) is due to the additional term $-B_1\bar{y}$. The effects of the uncompensated Δf on the image deformation are illustrated in Fig. 5. By comparing the geometric effects of equations (7), (12) and uncompensated Δf, it is obvious that the effect of equations (12) (Fig. 2(right)) is more distinctive from that of uncompensated Δf (Fig. 5). This helps to explain why equations (12) always deliver a lower correlation with Δf than equation (7).

In the practical experiments, equations (12) also provide a lower correlation with Δf than equation (7). The difference of the Δf calibration by using different formulae of in-plane distortion is not quite significant. This might be due to the quite small in-plane distortion evident with most digital cameras (Fraser, 1997).

All these results lead to the theoretical conclusion that equations (12) perform similarly to equation (7) and help to reduce the correlations between B_1 and Δf. Nevertheless, the amount of reduction depends on the magnitude of the in-plane distortion and the image configuration.

Conclusions

This paper has studied the high correlations between the principal point and the decentring distortion parameters, and between the principal distance and the in-plane distortion parameters, in close range photogrammetry.

Table 2. Self-calibration results using two in-plane distortion models. Correlations are given in the final column.

Experiments		$\hat{\sigma}_0(\mu m)$	$\Delta f(\mu m)$	R_{fB}
Simulation-10	Equation (7)	0·41	50·3	−0·81
	Equations (12)	0·41	50·0	−0·75
Simulation-4	Equation (7)	0·38	48·3	−0·78
	Equations (12)	0·38	50·2	−0·60
Practical-10	Equation (7)	0·34	46·1	−0·83
	Equations (12)	0·34	45·8	−0·80

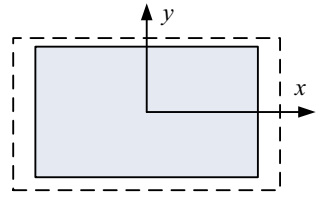

Fig 5. The effect of uncompensated $\Delta f > 0$ on geometric deformation.

It has been shown that the high correlations between the principal point and the decentring parameters are essentially caused by the polynomial representation of the Brown model. This is an intrinsic characteristic of camera interior orientation, in other words, the three IO parameters are invariably highly correlated with certain specific polynomial terms of the self-calibration models. These high correlations also occur in polynomial self-calibration models in aerial photogrammetry. It was further shown that, although high correlations do exist with the decentring parameters, the principal point can be reliably and precisely located in self-calibration, as long as the image configuration is appropriate. The bias of the principal point location caused by the high correlations is practically insignificant.

According to the correlation analyses, an alternative model of the in-plane distortion has been proposed. Compared with the conventional model, it can obtain similar or slightly refined calibration effects, and reduce the correlation with principal distance.

ACKNOWLEDGEMENTS

The authors would like to thank the anonymous reviewers for their valuable advice. Dipl.-Ing Alessandro Cefalu is appreciated for his help and discussion. The first author is grateful to the China Scholarship Council for the financial support during this work in Stuttgart, Germany.

REFERENCES

BROWN, D. C., 1966. Decentering distortion of lenses. *Photogrammetric Engineering*, 32(3): 444–462.

BROWN, D. C., 1971. Close-range camera calibration. *Photogrammetric Engineering*, 37(8): 855–866.

BROWN, D. C., 1972. Calibration of close-range cameras. *International Archives of Photogrammetry*, 19(5): 26 pages.

CLARKE, T. A. and FRYER, J. G., 1998. The development of camera calibration methods and models. *Photogrammetric Record*, 16(91): 51–66.

CLARKE, T. A., WANG, X. and FRYER, J. G., 1998. The principal point and CCD cameras. *Photogrammetric Record*, 16(92): 293–312.

EBNER, H., 1976. Self calibrating block adjustment. *Bildmessung und Luftbildwesen*, 44(4): 128–139.

FRASER, C. S., 1997. Digital camera self-calibration. *ISPRS Journal of Photogrammetry and Remote Sensing*, 52(4): 149–159.

FRASER, C. S. and AL-AJLOUNI, S., 2006. Zoom-dependent camera calibration in digital close-range photogrammetry. *Photogrammetric Engineering & Remote Sensing*, 72(9): 1017–1026.

GRUEN, A., 1978. Progress in photogrammetric point determination by compensation of systematic errors and detection of gross errors. *Nachrichten aus dem Karten- und Vermessungswesen,* II 36: 113–140.

LERMA, J. L. and CABRELLES, M., 2007. A review and analyses of plumb-line calibration. *Photogrammetric Record*, 22(118): 135–150.

LUHMANN, T., ROBSON, S., KYLE, S. and HARLEY, I. A., 2006. *Close Range Photogrammetry: Principles, Techniques and Applications*. Whittles, Caithness, Scotland. 510 pages.

STAMATOPOULOS, C. and FRASER, C. S., 2011. Calibration of long focal length cameras in close range photogrammetry. *Photogrammetric Record*, 26(135): 339–360.

TANG, R., FRITSCH, D., CRAMER, M. and SCHNEIDER, W., 2012. A flexible mathematical method for camera calibration in digital aerial photogrammetry. *Photogrammetric Engineering & Remote Sensing*, 78(10): 1069–1077.

WENG, J., COHEN, P. and HERNIOU, M., 1992. Camera calibration with distortion models and accuracy evaluation. *IEEE Transactions on Pattern Analysis and Machine Intelligence*, 14(10): 965–980.

WESTER-EBBINGHAUS, W., 1983. *Einzelstandpunkt-selbstkalibrierung: ein Beitrag zur Feldkalibrierung von Aufnahmekammern*, Deutche Geodaetische Kommision (DGK), Nr. 289.48 pages (in German).

WILEY, A. G. and WONG, K. W., 1995. Geometric calibration of zoom lenses for computer vision metrology. *Photogrammetric Engineering & Remote Sensing*, 61(1): 69–74.

ZHANG, Z., 2000. A flexible new technique for camera calibration. *IEEE Transactions on Pattern Analysis and Machine Intelligence*, 22(11): 1330–1334.
ZIEMANN, H., 1986. Thoughts on a standard algorithm for camera calibration. *International Archives of Photogrammetry and Remote Sensing*, 26(5): 85–93.

Résumé

Bien que le modèle d'auto-étalonnage de Brown ait été largement utilisé pendant plus de quarante ans en photogrammétrie rapprochée, l'impact négatif de fortes corrélations bien connues entre certains paramètres reste mal compris. Cet article présente une nouvelle étude de ces corrélations et montre qu'elles sont inhérentes au modèle de Brown en raison de sa nature polynomiale. Elles ont le même comportement que pour les paramètres additionnels en photogrammétrie aérienne. Malgré d'importantes corrélations entre les paramètres de distorsion de décentrement, le point principal peut être localisé par auto-étalonnage avec une exactitude quelques pixels si la configuration d'acquisition est appropriée. Un modèle alternatif de distorsion est proposé pour réduire la corrélation avec la distance focale.

Zusammenfassung

Auch wenn das Brown'sche Modell zur Selbstkalibration seit mehr als 40 Jahren in der Nahbereichsphotogrammetrie erfolgreich eingesetzt wird, sind die negativen Auswirkungen der bekannten hohen Korrelationen immer noch unklar. Daher präsentiert der folgende Beitrag eine methodische Studie zu diesem Problem. Es wird gezeigt, dass die hohen Korrelationen des Brown'schen Modells infolge der polynomialen Beschreibung system-immanent sind. Sie sind daher vergleichbar mit den Polynommodellen zusätzlicher Parameter zur Selbstkalibration in der Luftbildphotogrammetrie. Des Weiteren kann gezeigt werden, dass die Koordinaten des Bildhauptpunkts präzise (bis auf wenige Pixel) im Rahmen einer Selbstkalibration bestimmt werden können, auch wenn die Parameter der tangentialen Verzeichnung hochkorreliert sind. Ferner wird ein optionales Modell zur Kompensation der Verzeichnung vorgeschlagen, welches die Korrelation mit der Brennweite reduziert.

Resumen

Los parámetros de auto-calibración de Brown están siendo usados ampliamente en fotogrametría de objeto cercano desde hace cuarenta años, pero no están claros cuales son los efectos negativos de las conocidas y elevadas correlaciones entre sus parámetros. En este artículo se presenta un estudio y un punto de vista novedoso de estas correlaciones las cuales se demuestra que son inherentes en el modelo de Brown debido a su naturaleza polinomial; sucede exactamente lo mismo en el caso de los parámetros adicionales en fotogrametría aérea. A pesar de las grandes correlaciones existentes entre los parámetros de distorsión por descentramiento, usando una apropiada configuración de imágenes con parámetros de auto-calibración puede determinarse con precisión (de unos pocos píxeles) la posición del punto principal. Se propone un modelo alternativo de distorsiones en el plano focal, el cual ayuda a reducir la correlación de los parámetros de distorsión con la distancia focal.